Springer

KSME

Journal of Mechanical Science and Technology 26 (7) (2012) 2101~2105
www.springerlink.com/content/1738-494x
DOI 10.1007/s12206-012-0523-3

Material characterization of Inconel 718 from free bulging test at high temperature †

Joon-Tae Yoo[1,*], Jong-Hoon Yoon[1], Ho-Sung Lee[1] and Sung-Kie Youn[2]

[1]*Korea Aerospace Research Institute, Daejeon, 305-333, Korea*
[2]*Department of Mechanical Engineering, Korea Advanced Institute of Science and Technology, Daejeon, 305-701, Korea*

(Manuscript Received February 22, 2012; Revised March 16, 2012; Accepted April 10, 2012)

Abstract

Macroscopic superplastic behavior of metallic or non metallic materials is usually represented by the strain-rate sensitivity, and it can be determined by tensile tests in uniaxial stress state and bulging tests in multi axial stress state, which is the actual hot forming process. And macroscopic behavior of Non-SPF grade materials could be described in a similar way as that of superplastic materials, including strain hardening, cavity and so on. In this study, the material characterization of non-SPF grade Inconel 718 has been carried out to determine the material parameters for flow stress throughout free bulging test under constant temperature. The measured height of bulged plate during the test was used for estimation of strain-rate sensitivity, strain-hardening index and cavity volume fraction with the help of numerical analysis. The bulged height obtained from the simulation showed good agreement with the experimental findings. The effects of strain-hardening and cavity volume fraction factor for flow stress were also compared.

Keywords: Flow stress; Free bulging test; Hot gas forming; Inconel 718; Strain-hardening index; Strain-rate sensitivity

1. Introduction

Gas forming, including superplastic forming, provides a significant opportunity for forming complicated, lightweight components for aerospace application. This also increases part integrity by minimizing joining and joining problems. The most important advantage of using superplasticity is the simplicity and economy in tooling. But only restricted materials have superplastic characteristics.

At elevated temperature, the thermally activated component of the flow stress is usually expressed in a form of the power law:

$$\bar{\sigma} = K\dot{\bar{\varepsilon}}^{m}\bar{\varepsilon}^{n} \tag{1}$$

where $\bar{\sigma}$ is the effective flow stress, $\dot{\bar{\varepsilon}}$ is effective strain rate, K is a strength coefficient which depends on temperature and microstructure, m is the strain rate sensitivity and n is the work-hardening index. Hot working behavior of a material is strongly dependent on the processing parameters, i.e., temperature, strain rate and strain [1]. These parameters must be found by characterization to analysis and optimized forming procedures.

There are three representative test methods for the evaluation of superplastic characteristics: tensile test, cone cup test and free bulging test. Uniaxial tensile test is carried out under the uniaxial stress state and is relatively easier than other methods. However, multiaxial stress state occurs in the real hot gas forming situation, thus the strain rate sensitivity determined from the uniaxial tensile test might be different. Cone cup test was suggested in order to enhance the tensile test. The cone cup test [2, 3] uses a constant test pressure, and induces a constant and multiaxial stress state in the sheet. Therefore the test condition is similar to the real forming condition. However, it is difficult to exclude the friction effect which exists between the tool and workpiece and the friction condition might affect the material characterization. Free bulging test [4-6] was also suggested. It is similar to the cone cup test. But the test pressure changes continuously during the test in order to maintain constant strain rate. In this case, it is difficult to control the pressure to ensure a constant strain rate. In Refs. [7, 8], work-hardening index is calculated with the help of finite element method in free bulging test.

Inconel 718 is widely used nickel-base superalloy for aircraft applications to withstand a combination of high temperature, hot gas corrosion and high strength. But it is not easy to fabricate by conventional methods resulting in high cost and time. SPF grade Inconel 718 has already been characterized

*Corresponding author. Tel.: +82 42 860 2928, Fax.: +82 42 860 2233
E-mail address: jtyoo@kari.re.kr
† This paper was presented at the ICMR2011, Busan, Korea, November 2011. Recommended by Guest Editor Dong-Ho Bae

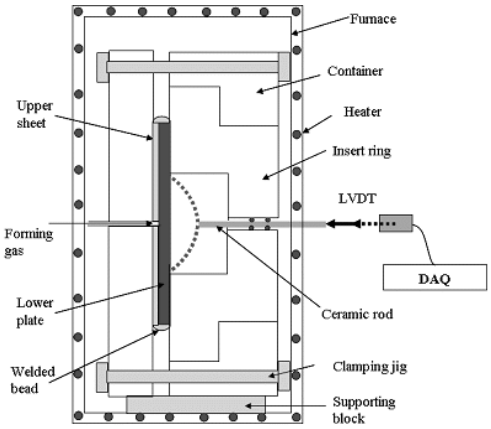

Fig. 1. Experimental setup for free bulging test.

by previous researches [9-13]. But characterization for non-SPF grade Inconel 718 is not common because of its low formability and restricted application for hot forming. If shape of product doesn't need superplastic deformation, hot gas forming can be applied for Inconel 718. It will save cost and manufacturing time. In this paper, material characterization of non-SPF grade Inconel 718 has been carried out using the free bulging test by constant pressure at high temperature. During the free bulging test, the height of the free bulged plate is measured according to time. Based on test data, material parameters for flow stress are calculated in bi-axial stress state. Strain-rate sensitivity and work-hardening index are considered as constant, but strength coefficient, *K,* is assumed as a function of strain to take into account microstructure evolution in large strain region. Finally, we find reasonable results for height at dome apex, thickness distribution after forming and deformed shape between experiment and analysis using obtained material parameters.

2. Free bulging test

A free bulging test using Inconel 718 was carried out under constant temperature, 980°C. The test pressure was considered for two cases of 5.0 MPa and 6.5 MPa. The supplied gas pressure increased up to the target pressure within 15 sec and was kept to be constant for 1800 sec. The displacement of the apex of bulged plate was measured according to time.

The experimental setup for the free bulging test is shown in Fig. 1. Diameter of the mould cavity is 106.0 mm and the fillet radius of inlet is 5.0 mm. The lower plate and the upper sheet for bulging were welded along the periphery to ensure air tightness. Gas pressure was supplied through the supply pipe welded to the upper sheet. Thickness of the bulged plate is 3.2 mm.

3. Characterization method

3.1 Theoretical consideration

Fig. 2 shows the process of free bulging. In this case the periphery of the sheet should be constrained so that radial displacement cannot occur, and inert gas is applied to the sheet surface.

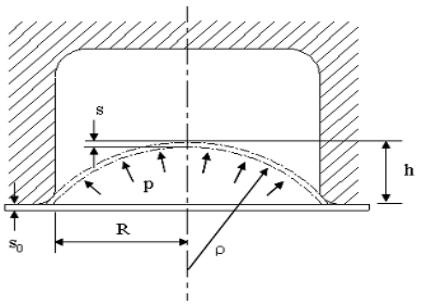

Fig. 2. Schematic representation of free bulging process.

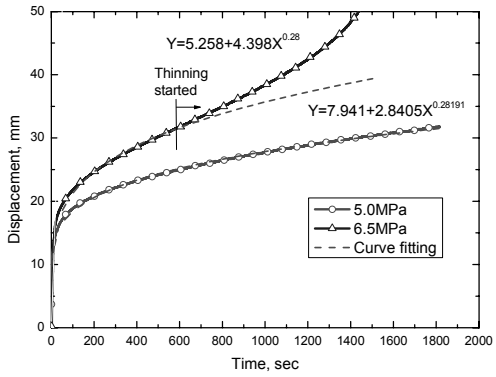

Fig. 3. Measured displacement and fitting functions.

Therefore, the sheet bulges into the mould cavity without friction. Each stress component can be expressed as a function of geometry parameters in Fig. 2 [14], and the relationship between the equivalent stress and strain rate will have the following form:

$$\frac{p\left(R^2+h^2\right)^2}{4hR^2s}=\Phi\left(\frac{-2h\dot{h}}{R^2+h^2}\right). \tag{2}$$

The only unknown variable is the height of the bulged sheet, h and $\dot{h}$ in Eq. (2). Thus if the height changes according to time are measured throughout the experiment, it is possible to obtain the strain rate and stress.

Fig. 3 shows the measured displacement at the apex. These height changes were fitted as an analytical function of time as shown in Fig. 3. But in case of 6.5 MPa pressure condition, bulged part is fractured during test at t = 1504 sec, h = 54.6 mm. Before fracture, the rate of change of displacement at the apex is increased suddenly because of local thinning near pole area. This area is excluded for the fitting function.

It is possible to calculate strain-rate and stress by substituting fitting equations into Eq. (2). If equivalent stress is only a function of the equivalent strain rate as shown in Eq. (3), K and m can be calculated.

$$\bar{\sigma}=K\dot{\bar{\varepsilon}}^{m}. \tag{3}$$

Table 1. Material parameters for Eq. (6).

Pressure (Mpa)	K (MPa)	m
5.0	251.0	0.143
6.5	398.0	0.190

The obtained strength coefficient and strain-rate sensitivity are summarized in Table 1.

3.2 Numerical consideration

If strain hardening effect is considered for flow stress calculation, Eq. (1) should be used. There are many previous works [1-6] to get material parameters for flow stress at high temperature. But in most cases the strain hardening effect was neglected to simplify the analysis and they showed reasonable results. In Refs. [7, 8], strain hardening effect was determined by adopting numerical method. In this chapter, the method proposed by Refs. [7, 8] is summarized.

The strain-rate sensitivity is determined from data obtained from free bulging test by

$$m = \frac{\ln(p_1 / p_2)}{\ln(t_2 / t_1)} \tag{4}$$

where t_1 and t_2 are the forming times necessary to obtain the same dome geometry at constant pressure p_1 and p_2, respectively. Employed assumptions for Eq. (4) are

- Material is isotropic and volume remains constant,
- Elastic strains are negligible,
- Sheet metal at any given instant is shaped as a part of a sphere subject to internal pressure,
- At the periphery, the sheet metal is rigidly clamped.

After strain-rate sensitivity is determined, n is calculated by minimizing the function Q:

$$Q(n) = \left(\frac{(\ln \tau)^N - (\ln \tau)^{EXP}}{(\ln \tau)^{EXP}} \right)_{p1}^2 + \left(\frac{(\ln \tau)^N - (\ln \tau)^{EXP}}{(\ln \tau)^{EXP}} \right)_{p2}^2 \tag{5}$$

where $\tau = t_{H=h1} / t_{H=h2}$ and $t_{H=h1}$, $t_{H=h2}$ are the forming time taken to reach the dome height, *h1* and *h2,* respectively, in constant pressure-forming process. $(\ln \tau)^N$ represents the value of the dimensionless time obtained from numerical simulation for a fixed value of n. For analysis, K is assigned an arbitrary value and n is made to vary in a suitable range. The value of n will be the one in correspondence to which the function $Q(n)$ assumes its minimum value.

Similarly, the parameter K is determined by minimizing the function F defined by

$$F(n) = \left(\frac{(t_{H=h1})^N - (t_{H=h1})^{EXP}}{(t_{H=h1})^{EXP}} \right)_{p1}^2 + \left(\frac{(t_{H=h1})^N - (t_{H=h1})^{EXP}}{(t_{H=h1})^{EXP}} \right)_{p2}^2 . \tag{6}$$

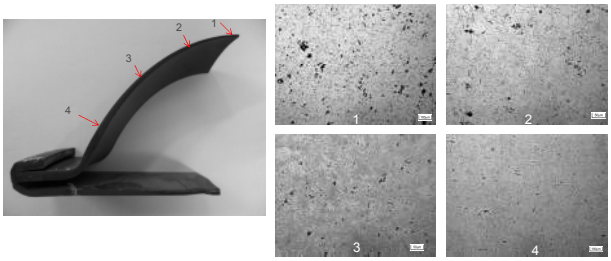

Fig. 4. Microstructure observation after free bulging test.

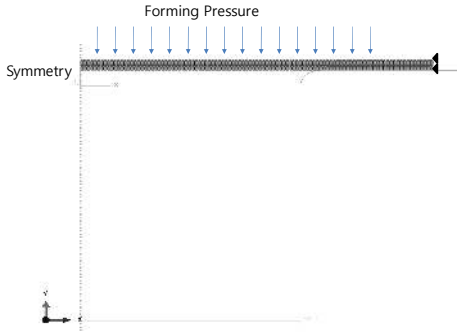

Fig. 5. Finite element model and boundary conditions.

3.3 Cavity volume fraction effect

In tensile testing at high temperature, cavities are easily observed in SPF grade Inconel 718 [10, 11]. In superplastic forming, Inconel 718 fails through a combination of necking, cavity growth and cavity interlinkage. And cavitation will be the dominant factor for failure at slow strain rate condition (1×10^{-4}/s) [12]. Cavitation may affect local thinning at pole before fracture is observed in an experiment. Cavitation effect for flow stress should be included to explain that.

Cavity volume fraction will depend on strain and is usually known as follows [15, 16]:

$$f = f_0 \exp(\eta \bar{\varepsilon}) \tag{7}$$

where f_0 is the extrapolated volume fraction of cavities at zero strain and η is the cavity growth rate parameter. In Ref. [16], cavity initiation strains are obtained according to hot working temperature.

After free bulging experiment, cavitations were found in bulged part as shown in Fig. 4. It shows cavity volume fraction is increased by moving to the pole direction. So cavity volume fraction factor is included in strength coefficient for analysis in the next chapter.

4. Numerical analysis for characterization

4.1 Analysis using material parameters excluding strain hardening

The material parameters in Table 1 are verified by finite element method. Analysis model is shown in Fig. 5.

Table 2. Material parameters for Eq. (1).

m	n	K (MPa)
0.237	0.0894	673.05

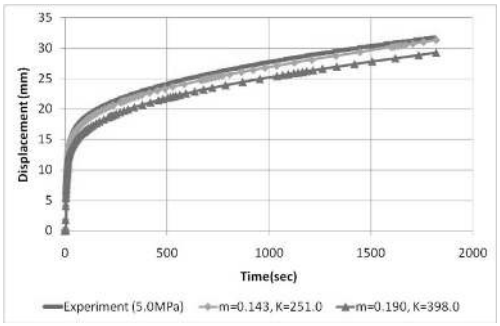

(a) p = 5.0 MPa

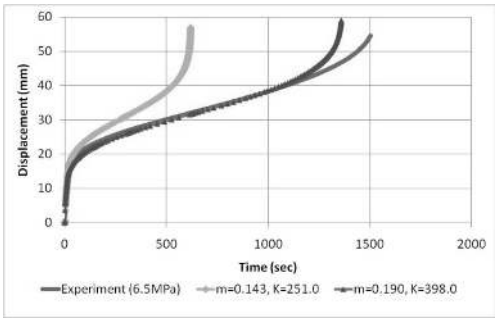

(b) p = 6.5 MPa

Fig. 6. Comparison of displacement: (a) p = 5.0 MPa; (b) p = 6.5 MPa.

ABAQUS/Standard is used for simulation. The element type used in the simulation is axisymmetric 4 node quadrilateral linear element. Fig. 6 shows the comparison with experiment in displacement change according to time at apex.

Material parameters show different values according to pressure condition, so all cases are analyzed for comparison. The analysis using material parameters obtained in same pressure condition has reasonable result with test. But if these parameters are applied to other pressure condition, it shows an entirely different result. So material parameters calculated in Table 1 are not general form but useful in that pressure condition.

4.2 Analysis using material parameters including strain hardening

The material parameters in Eq. (1) are obtained by the method described in Section 3.2 and shown in Table 2. Results are compared in Fig. 7. As shown in Fig. 7, displacement change is very similar to the experiment. But in 65 MPa pressure condition, local thinning before fracture is not explained with this model. As mentioned in Section 3.3, cavity volume fraction must be included to strength coefficient.

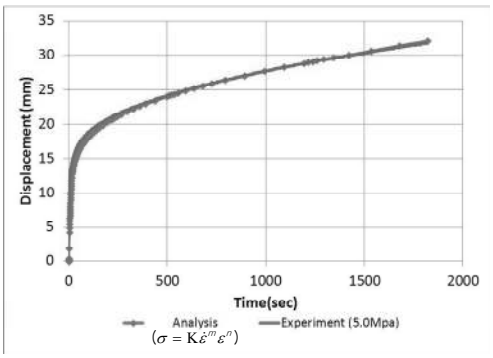

(a) p = 5.0 MPa

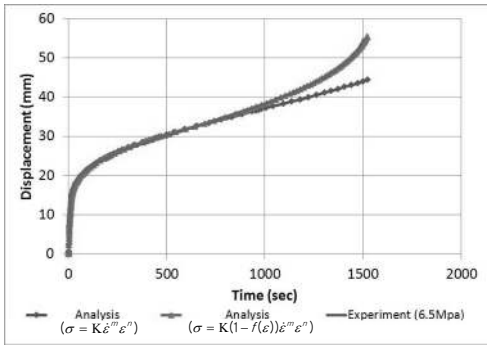

(b) p = 6.5 MPa

Fig. 7. Comparison of displacement: (a) p = 5.0 MPa; (b) p = 6.5 MPa.

4.3 Analysis using material parameters including strain hardening and cavity volume fraction

If cavity volume fraction is only function of strain, the flow stress equation can be expressed as

$$\sigma = K(1 - f(\varepsilon))\dot{\varepsilon}^m \varepsilon^n. \quad (8)$$

In this paper, cavity volume fraction, $f(\varepsilon)$, is assumed zero until the strain value reaches critical strain, ε_1 and it is increased with fixed slope after that.

In Fig. 7(b), separation between the result of the test and that of analysis starts about 500 sec. At that time, the strain value of the apex is 0.35. So critical strain is assumed as 0.35. Increasing rate of cavity volume fraction is found to minimize the error between analysis and experiment. The analysis result including cavity volume fraction is plotted together in Fig. 7(b) for comparison. In 5.0 Mpa pressure condition, maximum strain does not exceed critical strain. So cavity volume fraction is assumed as zero always.

Finally, deformed shape is also compared with test in Fig. 8. And thickness at the pole and bulged height is compared in Table 3. All results show good agreement with experiment after considering strain hardening and cavity volume fraction except deformed shape in 6.5 Mpa pressure condition (Fig. 8(b)). Deformed height and thickness at pole are almost the same, but the deformed shape has a little error. The contact

Table 3. Comparison of thickness and bulged height at apex.

	5 MPa		6.5 MPa	
	Thickness	Bulged height	Thickness	Bulged height
Experiment (mm)	2.39	31.8	0.82	54.6
Analysis (mm)	2.20	32.08	0.87	53.97
Error (%)	7.95	0.88	6.10	1.15

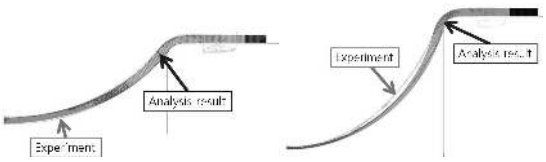

(a) p = 5.0 MPa (b) p = 6.5 MPa

Fig. 8. Comparison of deformed shape: (a) p = 5.0 MPa; (b) p = 6.5 MPa.

condition and fillet radius of the tool may cause this error during analysis. If this effect is studied, the degree of the precision of the analysis will be increased in deformed shape also.

5. Conclusions

From the free bulging test of Non-SPF grade Inconel 718, material parameters for flow stress at high temperature are determined including strain-rate sensitivity, strain hardening and cavity volume fraction. So the following conclusion can be obtained.

(1) Free bulging test using constant pressure can also be a material characterization method for Non-SPF grade material

(2) Inconel 718 used in this paper has low strain-rate sensitivity (0.237). So it doesn't have superplastic characteristics. If flow stress is described only by strain-rate, it cannot be a general form for flow stress.

(3) If strain-hardening effect is included for flow stress, it can be used for analysis with reasonable results before cavity volume fraction effect becomes dominant.

(4) Cavity volume fraction is assumed as a linear function and included in the strength coefficient. Analysis considering strain-rate sensitivity, strain hardening and cavity volume fraction for flow stress shows good agreement with experimental finding in displacement change during bulging, deformed shape and thickness at apex.

(5) Cavity volume fraction is estimated with the help of finite element analysis.

References

[1] H. S. Lee, J. H. Yoon, J. T. Yoo and W. H. Cho, Biaxial gas-pressure forming of a duplex stainless steel, *Advanced Materials Research,* 214 (2011) 374-377.

[2] R. J. Lederich, S. M. L. Sastry, M. Hayase and T. L. Mackay, Superplastic formability testing, *Journal of Metals*, August 1982, 16-20.

[3] A. K. Ghosh and C. H. Hamilton, On constant membrane stress test for superplastic metals, *Metallurgical Transactions A*, 11A (1980) 1915-1918.

[4] A. Dutta and A. K. Mukherjee, Superplastic forming: an analytical approach, *Material Science and Engineering*, A157 (1992) 9-13.

[5] G. C. Cornfield and R. H. Johnson, The forming of superplastic sheet metal, *International Journal of Mechanical Science*, 12 (1970) 479-490.

[6] F. Jovane, An approximate analysis of the superplastic forming of a thin circular diaphragm: Theory and Experiments, *International Journal of Mechanical Science*, 10 (1968) 403-427.

[7] G. Giuliano and S. Franchitti, The determination of material parameters from superplastic free-bulging tests at constant pressure, *International Journal of Machine Tools & Manufacture*, 48 (2008) 1519-1522.

[8] G. Giuliano and S. Franchitti, On the evaluation of superplastic characteristics using the finite element method, *International Journal of Machine Tools & Manufacture*, 47 (2007) 471-476.

[9] X. Han, L. Wu, H. Xia and R. Liu, Superplastic properties of Inconel 718, *Journal of Materials Processing Technology*, 137 (2003) 17-20.

[10] M. S. Yeh, C. W. Tsau and T. H. Chuang, Evaluation of the superplastic formability of SP-Inconel 718 superalloy, *Journal of Materials Engineering and Performance,* 5 (1996) 71-77.

[11] H. Lu, X. Jia, K. Zhang and C. Yao, Fine-grained pretreatment process and superplasticity for INCONEL 718 superalloy, *Materials Science and Engineering A,* 326 (2002) 382-385.

[12] Y. Huang and T. G. Langdon, Cavitation and failure in a fine-grained Inconel 718 alloy having potential superplastic properties, *Materials Science and Engineering A* 410-411 (2005) 130-133.

[13] M. W. Mahoney, Superplastic properties of alloy 718, *Superalloy 718-Metallurgy and Applications*, 1989.

[14] J.-H. Yoon, Y. M. Yi and H. S. Lee, Material characterization of duplex stainless steel by superplastic free bulging test, *6th EUROSPF Conference* (2008).

[15] Y. Takigawa, J. Velazquez Aguirre, E. M. Taleff and Kenji Higashi, Cavitation during grain-boundary-sliding deformation in an AZ61 magnesium alloy, *Materials Science and Engineering A,* 497 (2008) 139-146.

[16] S. L. Semiatin, V. Seetharamna, A. K. Ghosh, E. B. Shell, M. P. Simon and P. N. Fagin, Cavitation during hot tension testing of Ti-6Al-4V, *Materials Science and Engineering A*, 256 (1998) 92-110.

Joon-Tae Yoo has been working in the area of structure and material science for aerospace application at Korea Aerospace Research Institute since 1999.